Journal of Electrostatics 67 (2009) 301–306

Contents lists available at ScienceDirect

Journal of Electrostatics

journal homepage: www.elsevier.com/locate/elstat

Features of electrical discharges in air triggered by laser

Víctor March [a,*], Manuel Arrayás [b], José Luis Trueba [b], Joan Montanyà [a], David Romero [a], Glòria Solà [a], Daniel Aranguren [a]

[a] Electrical Engineering Department, Technological University of Catalonia (UPC), Colon, 1, Terrassa (Barcelona) 08222, Spain
[b] Universidad Rey Juan Carlos, Spain

ARTICLE INFO

Article history:
Received 12 September 2008
Received in revised form
12 December 2008
Accepted 23 January 2009
Available online 11 February 2009

Keywords:
Streamers
Laser-triggered discharges
Ionization
Electrical discharge
Multiphoton ionization

ABSTRACT

A numerical study of laser-triggered discharges in air at atmospheric pressure is presented for an ultraviolet laser in small gaps. Two models, one for the ionization of the air by the laser pulse and the second for the streamer evolution have been computed. From results of numerical simulations the influence of the laser parameters such as energy, pulse duration and beam radius is analyzed and electron distributions are obtained for different small gaps. Electric field, streamer velocity and evolution of the ionized volume are calculated by means of streamer simulations. This paper shows the main features of the laser-triggered discharges and also the importance of using numerical simulations in a laser-triggered experiment.

1. Introduction

Streamer formation and development have acquired great importance since its formulation by Raether, Meek and Loeb to explain the ionization phenomena between two charged electrodes. Townsend theory fails in the explanation of the ionization growth in electrical discharges in gases in which the product pressure × distance is higher than 200 mm Hg × cm [1].

Streamers play a crucial role in the electrical discharges as they are a necessary condition to complete the electrical breakdown in spark discharges.

The study of streamers has been extensively formulated through numerical simulations for different gases and pressures. Streamer simulations based on kinetic equations have been used to explain the development of the ionization path in the initial stages of the discharge. Nowadays streamer simulations are widely used to explain the ionization growth of an electrical discharge and can be found in many scientific papers and books (i.e. [2–4]).

On the other hand, the firsts experiments in laser-triggered discharges in laboratory are dated in the 1960s [5]. Laser pulses have the ability to ionize a volume of a gas when its intensity is higher than a threshold value depending on the laser system, the gas and pressure. For high intensity laser pulses ionized volumes grow in the gas due to the interaction of the laser with the matter.

Up to now high intensity laser systems have been developed and have the ability of guiding the electrical discharge due to the high ionized volume created in the gap. Actually some simulations using powerful laser beams are intended to create large filaments of ionized volume through the air (i.e. [6,7]).

This paper presents the main features of the electric discharges triggered by a laser beam through numerical simulations of the laser-created plasma and the subsequent streamer propagation in air at atmospheric pressure for small gaps.

2. Theory

2.1. Intensity threshold

A laser pulse with enough beam intensity has the ability of triggering electric discharges in a gaseous gap. The laser system required to ionize a volume of gas must be higher than 10^{10}W/cm^2 [8,9].

Laser beam intensity is a function of three parameters as shown in equation (1):

$$I_0 = \frac{2E}{\pi w \tau}\left[\frac{W}{m^2}\right] \tag{1}$$

E is the laser energy [J], w the beam radius [m] and τ the pulse duration [s].

* Corresponding author. Tel.: +34 620 07 68 36; fax: +34 93 739 82 36.
E-mail address: march@ee.upc.edu (V. March).

0304-3886/$ – see front matter © 2009 Elsevier B.V. All rights reserved.
doi:10.1016/j.elstat.2009.01.039

2.2. Laser ionization processes

The interaction of photons with a gas depends on the laser wavelength and the intensity of the beam. Three processes can be distinguished depending on the laser wavelength and intensity: Multiphoton Ionization, Inverse Bremsstrahlung and Tunnel Ionization.

The two first processes occur when the beam intensity is lower than 10^{14} W/cm^2 [10]. In this article Tunnel Ionization is not considered, as computed laser intensities are some orders of magnitude lower.

In Multiphoton Ionization process (MPI) multiple absorption of photons of the laser beam liberates an electron from the atom or molecule. The number of photons required to ionize a stable particle is:

$$n > \frac{U_I}{h\upsilon} = \frac{U_I}{E_{photon}} \tag{2}$$

where U_I is the ionization potential of the atom, h is the Planck's constant and υ the laser frequency. Laser beams in the UV (Ultraviolet) with higher photon energy than IR (Infrared) require a fewer number of photons to reach the ionization potential of the interacting atom to ionize it. For example, at 248 nm (UV) for a KrF excimer laser and 1064 nm (IR) for a Nd:YAG laser, the photon energies are around 5 and 1.2 eV respectively. For this reason MPI is the main process in the UV lasers.

In cascade ionization process, free initial electrons are accelerated via Inverse Bremsstrahlung. The free electrons absorb energy from the laser radiation field and start the cascade ionization process as they gain enough energy of the radiation field to impact a molecule and start a continuous process of ionization. An electron gains energy by Inverse Bremsstrahlung according to:

$$\frac{dE_e}{dt} = \frac{2Ie^2}{\varepsilon_o c m_e \upsilon^2}\upsilon_{ei} \tag{3}$$

where $E_e$is electron's energy, I laser beam's intensity, e the electron's charge, ε_o the vacuum's permittivity, c the speed of light, m_e electron's mass, υ the laser frequency and υ_{ei} electron–ion collision frequency.

In air, electrons must reach an energy of 12.2 eV (U_I of O_2) to start the cascade ionization process. Using ultraviolet laser beams, laser pulses longer than 60 ns are required to start cascade ionization process [6,11].

The threshold intensity to ionize the air is around 10^{10} W/cm^2 as previously indicated. This value depends on the laser's wavelength as ionization processes are different. In [12] the threshold value for IR (1.06 μm) wavelength is found to be $\approx 10^{11}$ W/cm^2. In [13] a laser intensity of 10^8 W/cm^{2}creates a measured electron density of 10^{11} cm^{-3} using a KrF (248 nm) excimer laser. This difference in the threshold value can be attributed to the ionization processes present in each laser system.

2.3. Laser propagation model

This section describes the ionization model for UV laser beams. The laser pulse is focused using a high transmission lens in UV (see Fig. 1). In the vicinity of the waist the intensity exceeds the threshold value and creates an ionized volume through Multiphoton Ionization process (MPI).

2.3.1. Ionization due to laser beam

When a laser beam with a wavelength of 248 nm is focused between the gap in a certain volume of air, the electron generation obtained by MPI is given [11] by equation (4):

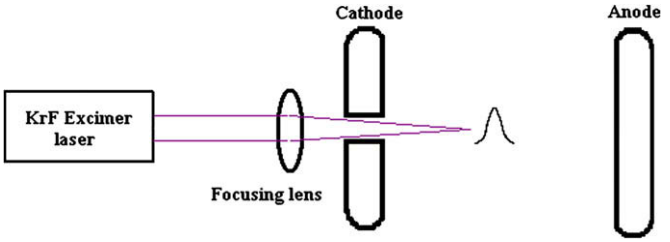

Fig. 1. Scheme of the laser-triggered discharge in a plane–plane gap.

$$\frac{dN_e}{dt} = (N_o - N_e)\sigma^{(n)} I(t)^n - \beta_{ep} N_e^2 - \nu_a N_e \tag{4}$$

where $\sigma^{(n)}$is the MPI coefficient for the nth order of ionization, β_{ep} is the recombination between electron and positive ion; and ν_a represents the attachment frequency.

From equation (4) the electron density can be obtained as a function of time. As the number of electrons grows in the gap due to MPI process, attachment and recombination take place reducing the electron density. The coefficients for Multiphoton Ionization, attachment and recombination are $\sigma^{(3)} = 3 \times 10^{-29}$ cm^6 s^2 J^{-3} [11], $\nu_a = 0.9 \times 10^8$ s^{-1} [14] and $\beta_{ep} = 5.98 \times 10^{-7}$ cm^3 s^{-1} [12] respectively for air at atmospheric pressure.

2.3.2. Power- loss

The absorption of photons per unit length is the most important loss present in the propagation of the beam in the present case of study as we focus in small gaps. The power-loss due to MPI is quantified in equation (5)

$$\frac{dP}{dz} = -\left(\frac{2}{\pi}\right)^2 3\hbar\omega N_o \sigma^{(n)} \frac{P^3}{w^4} \tag{5}$$

where $\hbar$ is the reduced Planck's constant [eV], ω the laser frequency [s^{-1}], N_o the density of neutral species [m^{-3}],$\sigma^{(n)}$ the Multiphoton Ionization coefficient [cm^{6}s^{2}J^{-3}], P beam power and w the beam radius.

2.3.3. Focusing of the laser beam

In order to reach intensities higher than 10^{10} W/cm^2 it is necessary to focus the laser beam. It is assumed that the laser pulse has a temporal and radial Gaussian distribution with TEM_{00} mode. The Gaussian beam is focused in atmospheric air considering that lens aberration is not present. It is used paraxial approximation at the vicinity of the focus to solve the value of the beam radius. The intensity at each position is then calculated as a function of the beam radius considering the Multiphoton Ionization losses which only occurs near the focal point.

2.4. Streamer simulation model

2.4.1. Balance equations

The model considered to simulate streamer development is based on kinetic theory [15,16], and the equations describing the evolution of the laser-created plasma:

$$\frac{\partial N_e}{\partial t} = \nabla_R(\mu_e N_e E + D_e \nabla_R N_e) + (\upsilon_i - \upsilon_a - \upsilon_{ep} N_p) N_e + S_{ph} \tag{6}$$

$$\frac{\partial N_p}{\partial t} = (\upsilon_i - \upsilon_{ep} N_p) N_e - \upsilon_{np} N_n N_p + S_{ph} \tag{7}$$

$$\frac{\partial N_n}{\partial t} = \upsilon_a N_e - \upsilon_{np} N_n N_p \tag{8}$$

where N_e, N_p and N_n are the electrons, positive ions and negative ions densities; E is the electric field; μ_e and D_e the electron mobility and diffusion; υ_i the impact ionization coefficient; υ_a, υ_{ep}, υ_{np} the dionization coefficients for attachment, and recombination for electron-positive ions and negative-positive ions respectively; S_{ph} is the photoionization term.

The evolution of the electric field is given by Poisson's equation:

$$\nabla_R E = \frac{e}{\varepsilon_o}(N_p - N_n - N_e) \tag{9}$$

where e is the electron's charge and ε_o the vacuum's permittivity.

Streamer model includes the most important ionization and deionization processes in air and neglects ion velocities being two orders of magnitude lower than electron velocities.

2.4.2. Coefficients

The streamer model includes the processes of impact ionization, photoionization, attachment and recombination. Mobility and diffusion are included for the calculation of the streamer evolution.

For the impact ionization coefficient ν_i the Townsend approximation is used [14],

$$\nu_i\left(s^{-1}\right) = \mu_e|\varepsilon|\alpha_o e^{-\varepsilon_o/|\varepsilon|} \tag{10}$$

in which, for air at atmospheric pressure,

$$\alpha_o\left(m^{-1}\right) = 1.14\cdot 10^6 \tag{11}$$

and

$$\varepsilon_o\left(\mathrm{V\,m^{-1}}\right) = 2.77\times 10^7 \tag{12}$$

Attachment coeficient according to [17]:

$$\upsilon_a\left(s^{-1}\right) = 1.22\times 10^8\left(\frac{N}{N_o}\right)e^{-42.3/\varepsilon_o} + 10^8\left(\frac{N}{N_o}\right)^2\frac{0.62+800\varepsilon_o^2}{1+10^3\varepsilon_o^2\left[\varepsilon_o\left(1+0.03\varepsilon_o^2\right)\right]^{1/3}} \tag{13}$$

Recombination coefficient as a rate for electron-positive (υ_{ep}) ion and negative-positive ion (υ_{np}):

$$\upsilon_{ep} = \upsilon_{np}\left(s^{-1}\right) = 1.42\times 10^{-17}, \tag{14}$$

electron diffusion and mobility can be approximated as [14,17]:

$$D\left(m^2/s\right) = 0.0827 \tag{15}$$

$$\mu_e\left(\mathrm{V^{-1}\,s^{-1}}\right) = 0.0549\ \mathrm{m^2} \tag{16}$$

In our study we consider that optical emissions from N_2 and N_2^+ molecules can ionize O_2 molecules. The photoionization rate, due to the fact that the number of photons emitted is physically proportional to the number of ions produced by impact ionization, is written as the following nonlocal source term [15,18,19],

$$S_{ph}(R) = S_o\int \upsilon_i(R')N_e(R')K_{ph}\left(|R-R'|\right)\mathrm{d}^3R'$$

Where S_o is given by

$$S_o = \frac{1}{4\pi}\frac{p_q}{p+p_q}\xi\left(\frac{\upsilon_*}{\upsilon_i}\right)\frac{1}{\ln(\chi_{max}/\chi_{min})}$$

In this expression, p_q is the quenching pressure of the singlet states of N_2, p is the gas pressure, ξ is the average photoionization efficiency in the interval of radiation frequencies relevant to the problem, υ_* is the effective excitation coefficient for N_2 state transitions from which the ionization radiation comes out (we take υ_*/υ_i to be a constant), and χ_{min} and χ_{max} are, respectively, the minimum and maximum absorption cross sections of O_2 in the relevant radiation frequency interval. The Kernel $K_{ph}(|R-R'|)$is written as [20]

$$K_{ph}(R) = \frac{\exp(-\chi_1 R)-\exp(-\chi_2 R)}{R^3},$$

In which $\chi_1 = \chi_{min}p_{O_2}$ and $\chi_1 = \chi_{max}p_{O_2}$, so that $\chi_1 < \chi_2$.

3. Results

The aim of the next simulations is to show, based on examples in small gaps, the properties and effects of the laser-triggered discharges. This work is only focused on small gaps with plane-plane electrode configuration as seen in Fig. 1 in which streamer discharges take place and no leader transition occurs as in large gaps.

3.1. Electron growth

As shown in equation (4) the electron density grows at the points where intensity is higher than 10^{10} W/cm^2. The laser intensity is higher as the beam approaches the focal point. Fig. 2a shows the intensity distribution of a laser pulse in a 2 cm gap. In this case the electron density after the laser pulse reaches a peak value of 1.6×10^{14} electrons cm^{-3} (Fig. 2b). The laser pulse has an energy of 1 mJ, a pulse duration of 5 ns (FWHM) and has been focused to 5 μm focal point.

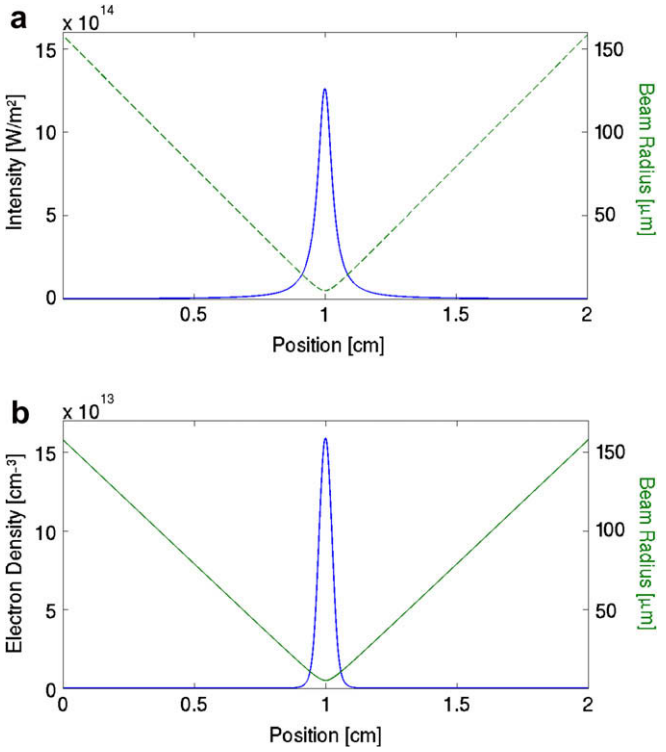

Fig. 2. (a) Intensity and beam radius calculated in a 2 cm gap in air at atmospheric pressure. (b) Calculated electron density and beam radius at same conditions. The beam radius at the focus is 5 μm.

3.2. Electron decay

The electron density grows as the laser intensity is applied and decays by attachment and recombination after the pulse application according to equation (1). After the laser pulse, if no electric field is applied the electron density decays as a function of time. In Fig. 3a, the evolution of the electron densities are plotted as a function of time for electron densities from 10^{11} to 10^{16} e^- cm^{-3}. An analysis of Fig. 3a shows that the decay becomes important after some tens of nanoseconds. That means that the reduction of the electron density has to be considered in a laser model when the duration of the laser pulse is not in the femtosecond or picosecond range. As shown in this figure the electron density decays approximately one order of magnitude 10 ns after the creation of these electron populations. In Fig. 3b the electron densities are plotted in a 2 cm gap corresponding to time $t = 0$, $t = 50$ and $t = 100$ ns after the laser pulse.

3.3. Electric field distortion

After the laser pulse, the electron density created starts to move due to the influence of the background electric field. The electric field becomes distorted as the electrons start to move to the anode (right side in Fig. 4). The head of the streamer moves to the anode and the electric field distortion reaches values of the order of the background field in the gap, as seen in Fig. 4.

According to the streamer theory [1], as the head of the electron avalanche reaches a density higher than 10^8 e^-/cm^3 the avalanche to streamer transition occurs and the background electric field becomes distorted. In Fig. 4 the electron density created by the laser pulse has a peak value around 10^{12} e^-/cm^3 . In this figure the electron density created by the laser pulse starts the streamer discharge and the ionized volume moves to the anode.

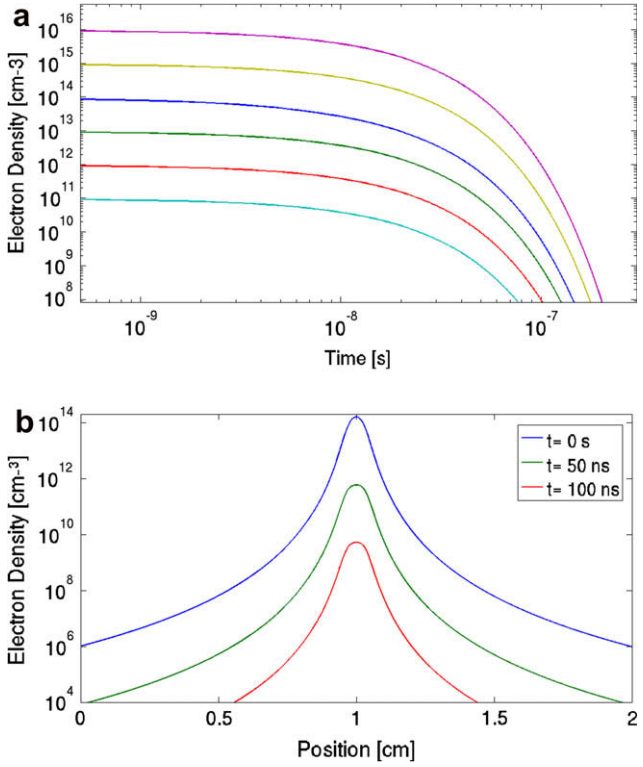

Fig. 3. (a) Temporal evolution of the electron density in air at atmospheric pressure for different initial values. (b) Electron densities for times $t = 0$ (blue), $t = 50$ ns (green) and $t = 100$ ns (red) after the laser pulse. [For interpretation of color in this figure legend the reader is referred to web version of the article.]

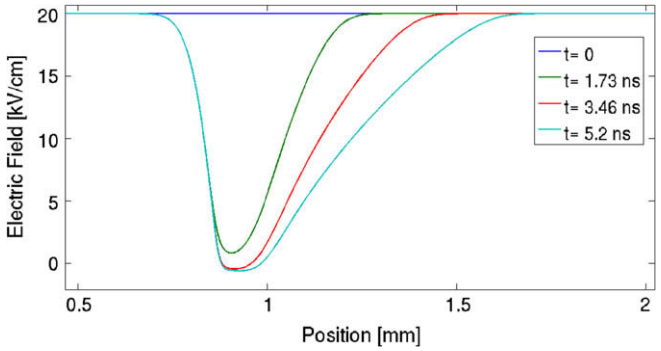

Fig. 4. Electric field distortions created in the gap during streamer development plotted in Fig. 5(b).

3.4. Reduction of the breakdown voltage

The reduction of the breakdown voltage with laser-triggered discharges is the main reason that makes this kind of discharges so attractive for scientists. As a laser is focused ionizing a volume of gas, the streamer can develop in some cases with electric fields lower than 10% the breakdown voltage without a laser [21].

As laser-triggered discharges have been applied to many different gases, gap configurations or voltage sources, using laser pulses with different wavelengths and intensities it is not possible to establish a percentage of the reduction in the breakdown voltage as it depends on each experiment.

In Fig. 5(a) and (b) the evolution of the electron densities for electric fields of 30 kV/cm and 20 kV/cm respectively is plotted for the first 5 ns. Anode directed streamers move at velocities of 1.1×10^7 cm/s and $9.4 \cdot 10^6$ cm/s respectively.

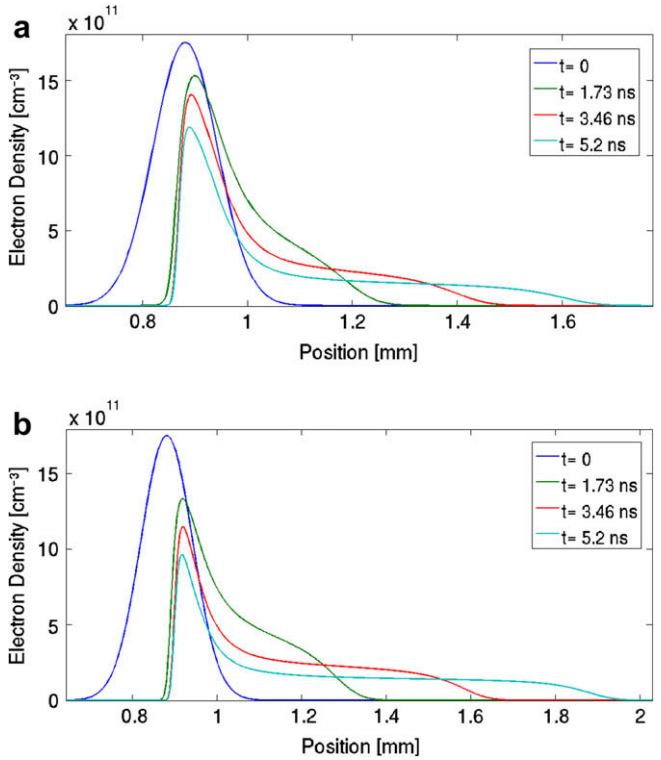

Fig. 5. Electron density profiles corresponding to times $t = 0$, $t = 1.73$ ns, $t = 3.46$ ns and $t = 5.2$ ns for (a) 30 kV/cm and (b) 20 kV/cm.

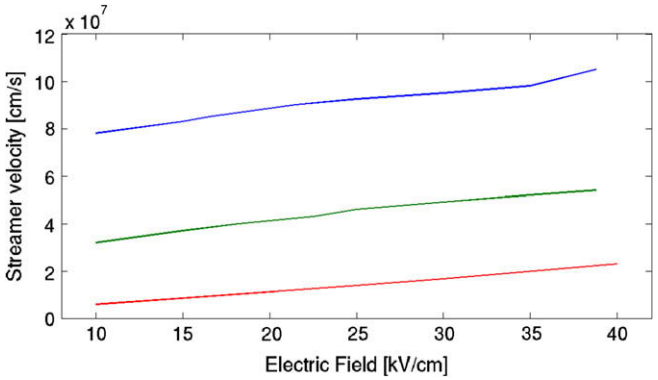

Fig. 6. Simulated streamer velocities for three different electron profiles and as a function of the background electric field.

3.5. Streamer velocity

The streamer velocity is mainly affected by two parameters in a triggered laser discharge: the background electric field and the electron population created by the laser.

Streamer velocities in air at atmospheric pressure normally vary between $10^7 - 10^9$ cm/s. The velocity of the streamer is affected by the length of the gap [22]. In numerical simulations the influence of the electric field and electron population can be calculated and analyzed. In Fig. 6 streamer velocities for different electron profiles and electric fields are plotted. As seen in Fig. 6, the streamer velocity not only depends on the electric field as it also changes with electrons's distribution.

3.6. Influence of the increasing laser energy

In most of the literature (i.e. [12,21,23]) the energy of the laser is varied mantaining constant the other laser parameters. In Fig. 7 various electron profiles calculated for different pulse energies are plotted. As can be seen in this figure, the increase of the laser energy changes the distribution and also the location of the electron peak.

In some cases, as laser energy is increased, no streamer can be observed before electrical breakdown, as occurred in [23] where an ionization path has been created in the whole gap by the laser pulse.

3.7. Influence of the focal radius

The intensity and electron distributions near the focal point are also influenced by the focal radius. As plotted in Fig. 8, for different

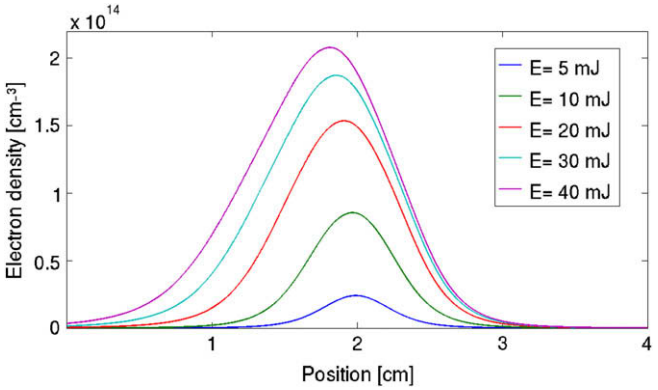

Fig. 7. Electron density profiles for laser energies of $E = 5$, 10, 20, 30 and 40 mJ; pulse duration is 5 ns (FWHM) and focal radius is 5 μm.

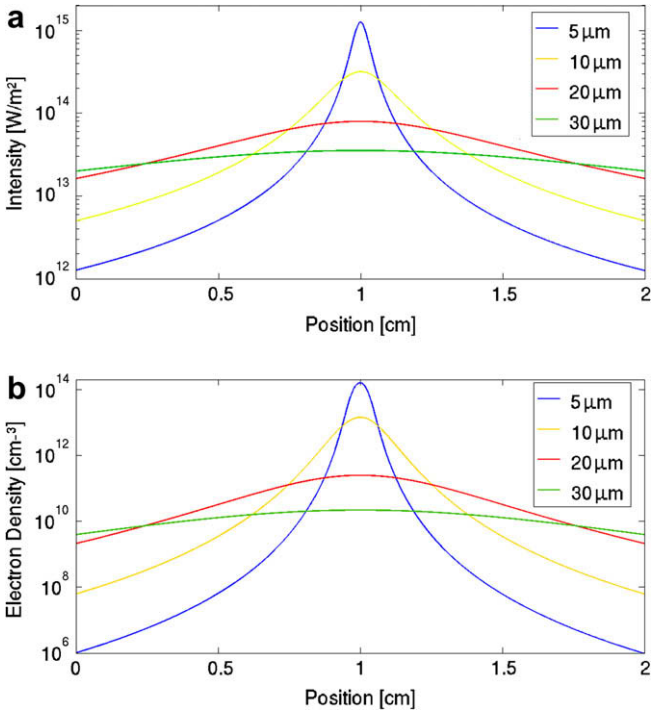

Fig. 8. (a) Calculated intensities in a 2 cm gap for different focal radius. (b) Electron densities calculated as a function of the focal radius and corresponding at the obtained in Fig. 8a.

focal radius the values of the intensity and the laser-created electrons differ in distribution and peak value. The effect of the initial profile of the created electrons on the subsequent streamer discharge is not negligible as indicated previously and create different ionized volumes. This influence can be seen in Fig. 8b. In this figure, electron's distributions of the laser for different focal radius are plotted. As seen in this figure, for a focal radius of 5 μm the electron density reaches a peak value of 10^{14} e^-/cm^3 but decreases to a density of 10^7 e^-/cm^3 at the end of the gap; In contrast, for a 30 μm focal radius the electron distribution reaches a value of 10^9 e^-/cm^3, homogenously distributed in the whole gap.

4. Conclusions

In this paper the main features of laser-triggered discharges have been presented through numerical simulations based on a laser ionization model for UV wavelengths and a streamer model using kinetic equations.

The laser ionization model gives the shape and value of initial electron distributions. From numerical results is concluded:

1. Intensities of the order of 10^{10} W/cm^2 are enough to ionize the air at atmospheric pressure with an ultraviolet laser and obtain electron densities of 10^{14} e^-/cm^3.
2. Electron decay plays an important role after some tens of nanoseconds, decreasing the electron density an order of magnitude.
3. Laser parameters such as energy or beam radius have a great influence on the initial plasma distribution.

In the case of the streamer model, the evolution of the laser-created plasma in a constant electric field has been calculated in air at atmospheric pressure. From Numerical simulations of laser-

created electrons the main parameters such as electron evolution, electric field and streamer velocity have been analyzed. For example, as the more attractive property for scientist as is the reduction of the breakdown voltage, numerical simulations of streamer evolution show that laser-triggered discharges can develop in an electric field lower than the required for normal breakdown.

For streamer simulation is concluded:

a. Laser-created plasma can evolve and ionize the air in electric fields lower than those required for breakdown without initial laser ionization.
b. Streamer velocities of the ionization front are of the same order as those usually calculated for streamers.
c. Laser-created plasma strongly distorts the electric field due to the high density of the ionized volume.

References

[1] J.M. Meek, A theory of spark discharge, Phys. Rev. 57 (1940) 722–728.
[2] C. Wu, E. Kunhardt, Formation and propagation of streamers in N_2 and N_2-SF_6 mixtures, Phys. Rev. A 37 (1998) 4396–4406.
[3] M. Arrayás, U. Ebert, Stability of negative ionization fronts: regularization by electric screening? Phys. Rev. E 69 (2004) 036214-1-10.
[4] M. Arrayás, U. Ebert, W. Hundshorfer, Spontaneous branching of anode-directed streamers between planar electrodes, Phys. Rev. Lett. 88 (2002) 174502.
[5] A.H. Guenther, J.R. Bettis, Laser-triggered megavolt switching, IEEE J. Quantum Electron. 3 (1967) 581–588.
[6] N. Khan, N. .Mariun, I. Aris, J. Yeak, Laser-triggered lightning discharge, New J. Phys. 4 (2002) 61.
[7] A. Couairon, L. Bergé, Light filaments in air for ultraviolet and infrared wavelengths, Phys. Rev. Lett. 88 (2002) 135003.
[8] T.X. Phuoc, Laser-induced spark ignition fundamental and applications, Opt. Lasers Eng. 44 (2006) 351–397.
[9] C.G. Morgan, Laser-induced breakdown of gases, Rep. Prog. Phys. 38 (1975) 621–665.
[10] B. La Fontaine, F. Vidal, Z. Jiang, C.Y. Chien, D. Comtois, A. Desparois, T.W. Johnson, J.-C. Kieffer, H. Pépin, H.P. Mercure, Filamentation of ultrashort pulse laser beams resulting from their propagation over long distances in air, Phys. Plasmas 6 (1999) 1615–1621.
[11] J. Schwarz, J.C. Diels, Analytical solutions for uv filaments, Phys. Rev. A 65 (2001) 013806.
[12] D.W. Koopman, K.A. Saum, Formation and guiding of high-velocity electrical streamers by laser-induced ionization, J. Appl. Phys. 44 (1973) 5328–5336.
[13] J. Sasaki, S. Kubodera, R. Ozaki, T. Uchiyama, Characteristics of interelectrode flashover in air with the existence of a weakly ionized plasma channel induced by a KrF laser (248 nm), J. Appl. Phys. 60 (1986) 3845–3849.
[14] Yu.P. Raizer, Gas Discharge Physics, Springer, Berlin, 1991.
[15] M. Arrayás, M.A. Fontelos, J.L. Trueba, Photoionization effects in ionization fronts, J.Phys. D: Appl. Phys. 39 (2006) 5176–5182.
[16] M. Arrayás, J.L. Trueba, Investigations of pre-breakdown phenomena: streamer discharges, Contemp. Phys. 46 (2005) 265–276.
[17] X.M. Zhao, J.-C. Diels, C.Y. Wang, J.M. Elizondo, Femtosecond ultraviolet laser pulse induced lightning discharges in gases, IEEE J. Quant. Elect. 31 (1995) 599–612.
[18] N. Liu, V.P. Pasko, Effects of photoionization on propagation and branching of positive and negative streamers in Sprites, J. Geophys. Res. 109 (2004) 1–17.
[19] G.V. Naidis, On photoionization produced by discharges on air, Plasma Sources Sci. Technol. 15 (2006) 253–255.
[20] M.B. Zhelezniak, A.Kh. Mnatsakanian, S.V. Sizykh, Photoionization of nitrogen and oxygen mixtures by radiation from a gas discharge, High Temp. 20 (1982) 357–362.
[21] N.J. West, I.R. Jandrell, A. Forbes, Preliminary investigation into laser-high voltage interaction in the case of the streamer-to-leader process using a high power CO_2 laser, in: Proc. Of the 28th International Conference on Lightning Protection, Kanazawa, 2006, pp. 620–624.
[22] E.M. Bazelyan, Yu.P. Raizer, Spark discharge. Boca Raton, New York, 1998.
[23] M. Akyuz, M. Rahman, A. Larsson, V. Cooray, A. Franke, Characteristics of laser-triggered electric discharges in air, IEEE Trans. Dielec. Elec. Insul. 12 (2005) 1060–1070.